IEEE Access
Multidisciplinary | Rapid Review | Open Access Journal

Received November 13, 2019, accepted December 7, 2019, date of publication December 19, 2019,
date of current version December 31, 2019.

Digital Object Identifier 10.1109/ACCESS.2019.2960840

Fast Simulations of Electromagnetic Scattering From One-Dimensional Rough Surface Over a Frequency Band Using Hybrid AMCBFM-Maehly Method

ANQI WANG[1], JINGJING WANG[2], ZHIXIANG HUANG[1], LIXIN GUO[2], (Senior Member, IEEE), AND TIEZHEN JIANG[1]

[1]Key Laboratory of Intelligent Computing and Signal Processing, Ministry of Education, Anhui University, Hefei 230039, China
[2]School of Physics and Optoelectronic Engineering, Xidian University, Xi'an 710071, China

Corresponding author: Zhixiang Huang (zxhuang@ahu.edu.cn)

This work was supported by the National Natural Science Foundation of China (Grant No. 61871457, No. 61971002, No. 61971001, No. 61722101), by the Natural Science Foundation of Anhui Province (Grant No. 1608085QF141, 1608085MF135), and by the Provincial Program of Natural Science of Anhui Higher Education (Grant No. KJ2019A0028).

ABSTRACT In this paper, the hybrid AMCBFM-Maehly method is presented to fast simulate the electromagnetic scattering from one-dimensional rough surface over a frequency band. In this approach, the traditional Maehly technique is applied to get the rational function of the induced electric current along the rough surface over a frequency band. The adaptive modified characteristic basis function method (AMCBFM) is utilized to fast compute the induced electric current along the rough surface at the Chebyshev nodes of the Maehly technique. Moreover, in the AMCBFM, the size of the matrix is reduced. And a current criterion is defined to adaptively halt the order of the characteristic basis functions (CBFs). The validity and efficiency of the hybrid AMCBFM-Maehly are assessed by comparing the numerical results of the hybrid AMCBFM-Maehly with the method of moments (MoM). The hybrid AMCBFM-Maehly can effectively reduce the size of the matrix, and it costs nearly half the CPU time used by the MoM. Moreover, by comparing with the traditional Maehly technique, the hybrid AMCBFM-Maehly costs less time. Additionally, in most cases, the first order of the CBFs of the hybrid AMCBFM-Maehly is sufficient for this result.

INDEX TERMS Adaptive modified characteristic basis function method, Maehly approximation, rough surface, frequency band, method of moments.

I. INTRODUCTION

Electromagnetic (EM) scattering from rough surface has been widely studied and applied in areas of target detection, marine communication, and stealth technology. In recent years, the EM scattering from rough surface over a frequency band has attracted more and more attentions for the application of the wideband or the ultra-wideband radars with high range resolution. The method of moments (MoM) is one of the mostly popular numerical methods for high accuracy and non-additional boundary condition [1]–[4]. However, the use of the MoM is time consuming because of the repeated calculations at every frequency. Several algorithms based on the MoM have been proposed to quickly simulate the EM scattering over a frequency band, such as, the asymptotic waveform evaluation (AWE) techniques [5]–[8], the model-based parameter estimation (MBPE) [9]–[11] and the Maehly approximation [12]–[16]. Comparing with the AWE and the MBPE, high derivates are not required and the accuracy can be controllable in the Maehly technique. In previous works of our research teams, the Maehly technique has been applied to simulate the EM scattering from the rough surface over a frequency band [14]–[16]. However, in these works, the MoM is used to get the induced electric current along the rough surface at the Chebyshev nodes. The dimension of the matrix is $N \times N$, where N represents the number of unknowns.

The associate editor coordinating the review of this manuscript and approving it for publication was Wei E. I. Sha.

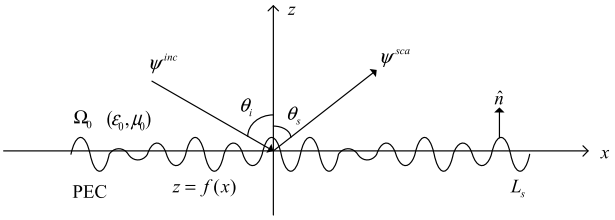

FIGURE 1. Geometric model of the EM scattering from a PEC rough surface.

When solving the problem with many unknowns, it will be very time-consuming.

In this paper, the adaptive modified characteristic basis function method (AMCBFM) [17] is utilized to fast compute the induced electric current along the rough surface at the Chebyshev nodes of the Maehly technique. And the approach is defined as the hybrid AMCBFM-Maehly method. The AMCBFM has been proposed by our teams to fast simulate the bistatic scattering from the rough surface [18]. In the AMCBFM, the N segments of the rough surface are firstly divided into M cells, every cell contains $N_i (i = 1, 2, \cdots, M)$ segments, where N_i represents the segments of i_{th} cell, and $N_1 + N_2 + \cdots + N_M = N$. The self-interaction of each cell is considered to generate the primary characteristic basis functions (PCBFs). Then the coefficients of the PCBFs are defined. And the primary total current of each cell is obtained by combining the PCBFs and the coefficients. In addition, the mutual coupling effect of the subcells is considered to build the secondary characteristic basis functions (SCBFs). And the secondary total current is composed by the SCBFs and its coefficients. So, in the AMCBFM, only the self-interaction impedance matrix with $N_i \times N_i$ are handled. It is readily seen that the AMCBFM can effectively reduce the size of the matrix. And in the AMCBFM, a current criterion is applied to adaptively halt the order of the SCBFs.

The remainder of this paper is organized as follows. In Section II, the theoretical formulations of the MoM, the traditional Maehly approximation, and the hybrid AMCBFM-Maehly method are exhibited in detail. In Section III, the validity and efficiency of the hybrid AMCBFM-Maehly are assessed by comparing with results of the MoM and the traditional Maehly technique. Section IV presents a summary of this paper and further plans on this topic.

II. THEORETICAL FORMULATIONS

A. EM SCATTERING from A ROUGH SURFACE USING THE MoM

Assume that a tapered plane wave ψ^{inc} incidents upon a PEC rough surface, as shown in Fig. 1, where $z = f(x)$ is a Gaussian rough surface with a simulated length L_s. θ_i and θ_s are the incident angle and the scattered angle, respectively. Space Ω_0 with the relative permittivity ε_0 and the relative permeability μ_0 is the incident space. Here, space Ω_0 is assumed to be the free space, i.e.,$\varepsilon_0 = 1$, and $\mu_0 = 1$. ψ^{sca} represents the scattered wave in the space Ω_0. The position vector is $\boldsymbol{r} = x\hat{\boldsymbol{x}} + z\hat{\boldsymbol{z}}$.

For a Horizontal (H) polarized incident wave, the surface integral equation for this scattering problem is [19]

$$\psi^{inc}(\boldsymbol{r}) = \int_s ds' G(\boldsymbol{r}, \boldsymbol{r}') \hat{\boldsymbol{n}}' \cdot \nabla \psi^t(\boldsymbol{r}') \tag{1}$$

where S denotes the interface of the Gaussian rough surface, $\hat{\boldsymbol{n}}'$ is the unit normal vector of the rough surface, $G(\boldsymbol{r}, \boldsymbol{r}') = \frac{i}{4} H_0^{(1)}(k_0 |\boldsymbol{r} - \boldsymbol{r}'|)$ is the two-dimensional Green's function in the space Ω_0, k_0 is the wavenumber in the space Ω_0, and $\psi^t(\boldsymbol{r}') = \psi^{inc}(\boldsymbol{r}') + \psi^{sca}(\boldsymbol{r}')$ represents the total wave including the incident wave and the scattered wave in the space Ω_0.

For the Vertical (V) incidence, the surface integral equation for this problem is [19]

$$\psi^{inc}(\boldsymbol{r}) = \frac{1}{2}\psi^t(\boldsymbol{r}) - \int_S ds' \psi^t(\boldsymbol{r}') \hat{\boldsymbol{n}}' \cdot \nabla G(\boldsymbol{r}, \boldsymbol{r}') \tag{2}$$

By using the MoM with the pulse basis functions and the point matching technique, the integral equations (1) and (2) can be discretized into the following matrix equations

$$\bar{\boldsymbol{A}} \cdot \boldsymbol{U} = \boldsymbol{b} \tag{3}$$

$$\bar{\boldsymbol{B}} \cdot \boldsymbol{I} = \boldsymbol{V} \tag{4}$$

The elements of the impedance matrix $\bar{\boldsymbol{A}}$ and $\bar{\boldsymbol{B}}$ in detail are

$$A_{mn} = \begin{cases} \frac{i\Delta x}{4} H_0^{(1)}(k_0 |\boldsymbol{r}_m - \boldsymbol{r}_n|), & m \neq n \\ \frac{i\Delta x}{4}\left[1 + i\frac{2}{\pi}\ln(\frac{\gamma k_0}{4e}\Delta l_m)\right], & m = n \end{cases} \tag{5}$$

$$B_{mn} = \begin{cases} -\Delta x \frac{1}{4} H_1^{(1)}(k_0 |\boldsymbol{r}_m - \boldsymbol{r}_n|), & m \neq n \\ \frac{1}{2} - \frac{\Delta x}{4\pi} \frac{f''(x_m)}{1+(f'(x_m))^2}, & m = n \end{cases} \tag{6}$$

here, $\frac{\gamma}{4e} = 0.163805$, and $\Delta l_m = \Delta x\sqrt{1 + (f'(x_m))^2}$. Subscripts m and n are the evaluation point and the source point along the rough surface, respectively. The elements of the right vector $\boldsymbol{b}$ and $\boldsymbol{V}$ are $\psi^{inc}(\boldsymbol{r}_m)$, and the left vectors $\boldsymbol{U}$ and $\boldsymbol{I}$ are the unknowns which represents the induced current along the rough surface.

B. THEORETICAL FORMULATIONS OF THE TRADITONAL MAEHLY APPROXIMATION

Analyzing equations (3) and (4), the two equations can be rewritten as

$$\bar{\boldsymbol{Z}}(k) \cdot \boldsymbol{J}(k) = \boldsymbol{V}(k) \tag{7}$$

where $\bar{\boldsymbol{Z}}$ is the impedance matrix with the dimensions $N \times N$, the right vector $\boldsymbol{V}$ with the dimensions $N \times 1$, the dimensions of the left vector $\boldsymbol{J}$ are $N \times 1$, and N is the number of the discrete segments along the rough surface.

From equation (7), it is readily seen that one must repeat the computations at every frequency to simulate the EM scattering over a frequency band. In this Maehly approximation,

the wavenumber $k \in [k_a, k_b]$ corresponding to the given frequency band $f \in [f_a, f_b]$ is firstly defined as

$$k = \frac{1}{2}\left[\tilde{k}(k_b - k_a) + (k_b + k_a)\right] \tag{8}$$

with $\tilde{k} \in [-1, 1]$.

Using the Chebyshev approximation, the element of the left vector $\boldsymbol{J}$ at the given frequency f can be given by

$$J_n(k) \approx \frac{1}{2}c_n^0 + \sum_{l=1}^{Q} c_n^l T_l(\tilde{k}) \tag{9}$$

here Q represents the total number of Chebyshev polynomials, and the unknown coefficients c_n^l are

$$c_n^l = \frac{2}{Q+1}\sum_{i=0}^{Q} J_n(k_i)T_l(\tilde{k}_i) \tag{10}$$

where $T_0(x) = 1$, $T_1(x) = x$ and $T_{n+1}(x) = 2xT_n(x) - T_{n-1}(x)$ are the Chebyshev polynomials, $\tilde{k}_i (i = 0, 1, \cdots, Q)$ are the Chebyshev nodes for $T_{Q+1}(\tilde{k}) = 1$, with

$$\tilde{k}_i = \cos(\frac{i+0.5}{n+1}\pi) \quad (i = 0, 1, \ldots, Q) \tag{11}$$

and $k_i \in [k_a, k_b]$ can be obtained by substituting $\tilde{k}_i$ into (8).

To improve the accuracy of the numerical simulation, equation (9) is recognized as a rational function, which is named as the Maehly approximation,

$$J_n(k) = \frac{\sum_{i=1}^{L} a_n^i T_i(\tilde{k})}{1 + \sum_{j=1}^{M} b_n^j T_j(\tilde{k})} \tag{12}$$

where the integers L and M are the orders of the zero expansions and the pole expansions, respectively, with $L + M = Q$. Combining (12), (9) and using the identity

$$T_p(x)T_q(x) = \frac{1}{2}(T_{p+q}(x) + T_{|p-q|}(x)) \tag{13}$$

The coefficients a_n^i and b_n^j can be yielded (15), as shown at the bottom of the next page.

$$\begin{cases} a_n^0 = \frac{1}{2}c_n^0 + \frac{1}{2}\sum_{j=1}^{M} b_n^j c_n^j \\ a_n^i = c_n^i + \frac{1}{2}\sum_{j=1}^{M} b_n^j (c_n^{j+1} + c_n^{|j-i|}),\ i = 1, 2, \ldots, L \end{cases} \tag{14}$$

After obtaining the coefficients a_n^i and b_n^j, one can acquire the induced current at any frequency within the whole frequency band.

The error of the Maehly approximation is defined as

$$RMSE = \frac{\left\| BSC_{Maehly} - BSC_{MoM} \right\|_2}{\left\| BSC_{MoM} \right\|_2} \tag{16}$$

where BSC_{MoM} represents the back scattering coefficient (BSC) over the frequency band $f \in [f_a, f_b]$ obtained by the MoM, BSC_{Maehly} denotes the interpolated broadband BSC results calculated by the Maehly technique, and $\|\cdot\|_2$ is the L_2 norm.

C. THEORETICAL FORMULATIONS OF THE HYBRID AMCBFM-MAEHLY METHOD

From the Maehly approximation, it is obviously found that if the MoM is used to get the unknowns $J_n(k_i)$ in equation (10), the traditional Maehly approximation is still limited by the MoM. In this paper, the AMCBFM is introduced to get the unknowns $J_n(k_i)$, and this approach is defined as the hybrid AMCBFM-Maehly method.

Similar as the AMCBFM [18], in the hybrid AMCBFM-Maehly method, the N segments of the rough surface are firstly divided into M cells, every cell contains $N_i (i = 1, 2, \cdots, M)$ segments, and $N_1 + N_2 + \cdots + N_M = N$. It is necessary to note that the length of every cell is at least 0.15λ to prove the continuity of current between sub-cells. Since then equation (7) can easily be recognized as equation [20]

$$\begin{bmatrix} \bar{\boldsymbol{Z}}_{11} & \bar{\boldsymbol{Z}}_{12} & \cdots & \bar{\boldsymbol{Z}}_{1M} \\ \bar{\boldsymbol{Z}}_{21} & \bar{\boldsymbol{Z}}_{22} & \cdots & \bar{\boldsymbol{Z}}_{2M} \\ \vdots & \vdots & \vdots & \vdots \\ \bar{\boldsymbol{Z}}_{M1} & \bar{\boldsymbol{Z}}_{M2} & \cdots & \bar{\boldsymbol{Z}}_{MM} \end{bmatrix} \begin{bmatrix} \boldsymbol{J}_1^{Tot} \\ \boldsymbol{J}_2^{Tot} \\ \vdots \\ \boldsymbol{J}_M^{Tot} \end{bmatrix} = \begin{bmatrix} \boldsymbol{V}_1 \\ \boldsymbol{V}_2 \\ \vdots \\ \boldsymbol{V}_M \end{bmatrix} \tag{17}$$

where, $\bar{\boldsymbol{Z}}_{ij} (i = 1, 2, \cdots, M; j = 1, 2, \cdots, M)$ represents the mutual impedance matrix of the i_{th} cell and the j_{th} cell with the dimensions $N_i \times N_j$. $\boldsymbol{J}_i^{Tot}$ is the total current of the i_{th} cell, which represents the induced current along the i_{th} cell. And the right form $\boldsymbol{V}_i$ indicates the incident wave upon the i_{th} cell.

(1) The primary total current $\boldsymbol{J}_i^{Tot(p)}$

For the $i_{th} (i = 1, 2, \cdots, M)$ cell, only the self-interaction is considered to generate the PCBFs $\boldsymbol{J}_i^p$

$$\bar{\boldsymbol{Z}}_{ii} \cdot \boldsymbol{J}_i^p = \boldsymbol{V}_i (i = 1, 2, \cdots, M) \tag{18}$$

where $\bar{\boldsymbol{Z}}_{ii}$ is the self-interaction impedance matrix of the i_{th} cell, $\boldsymbol{J}_i^p$ and $\boldsymbol{V}_i$ are the PCBFs and the incident wave vector of the i_{th} cell, respectively. Using the lower upper (LU) decomposition technique, one can obtain the PCBFs $\boldsymbol{J}_i^p$. The lower and the upper triangular matrices of $\bar{\boldsymbol{Z}}_{\boldsymbol{ii}}$ are obtained and saved for obtaining the SCBFs.

Assuming the total current $\boldsymbol{J}_i^{Tot}$ is only from the PCBFs, it is called as the primary total current $\boldsymbol{J}_i^{Tot(p)}$, and it can be defined as

$$\boldsymbol{J}_i^{Tot(p)} = a_{pi}^{(p)} \boldsymbol{J}_i^p \tag{19}$$

where $a_{pi}^{(p)}$ is the coefficient of the PCBFs.

Taking equation (19) into equation (17), one can obtain

$$\begin{bmatrix} \bar{\boldsymbol{Z}}_{11} & \bar{\boldsymbol{Z}}_{12} & \cdots & \bar{\boldsymbol{Z}}_{1M} \\ \bar{\boldsymbol{Z}}_{21} & \bar{\boldsymbol{Z}}_{22} & \cdots & \bar{\boldsymbol{Z}}_{2M} \\ \vdots & \vdots & \vdots & \vdots \\ \bar{\boldsymbol{Z}}_{M1} & \bar{\boldsymbol{Z}}_{M2} & \cdots & \bar{\boldsymbol{Z}}_{MM} \end{bmatrix} \begin{bmatrix} \boldsymbol{J}_1^{Tot(p)} \\ \boldsymbol{J}_2^{Tot(p)} \\ \vdots \\ \boldsymbol{J}_M^{Tot(p)} \end{bmatrix} = \begin{bmatrix} \boldsymbol{V}_1 \\ \boldsymbol{V}_2 \\ \vdots \\ \boldsymbol{V}_M \end{bmatrix} \tag{20}$$

Then, by multiplying equation (20) with $\left[\boldsymbol{J}_i^p\right]^H$, where $N = 4096$ is the conjugate transpose of $\boldsymbol{J}_i^p$, yield (21), as shown at the bottom of the this page.

(2) The first total current $\boldsymbol{J}_i^{Tot(1)}$

It is obviously found that the mutual coupling effect of the sub cells is neglected in equation (18), and thus $\boldsymbol{J}_i^{Tot(p)}$ is not accurate.

Considering the mutual coupling effect of the sub cells to build the SCBFs, for the $i_{th}(i = 1, 2, \cdots, M)$ cell, the first order of the SCBFs $\boldsymbol{J}_i^{S^1}$ is defined as

$$\bar{\boldsymbol{Z}}_{ii}\boldsymbol{J}_i^{S^1} = -\sum_{i=1,j=1,j\neq i}^{M} \left|a_{pj}^{(p)}\right| \bar{\boldsymbol{Z}}_{ij}\boldsymbol{J}_j^p \tag{22}$$

where $\boldsymbol{J}_i^{S^1}$ is the first order of SCBFs of the i_{th} cell.

The first total current $\boldsymbol{J}_i^{Tot(1)}$ is defined as

$$\boldsymbol{J}_i^{Tot(1)} = a_{pi}^{(1)}\boldsymbol{J}_i^p + a_{1i}^{(1)}\boldsymbol{J}_i^{S^1} \tag{23}$$

where $a_{pi}^{(1)}$ and $a_{1i}^{(1)}$ are the coefficients of the PCBFs and the first order of SCBFs, respectively.

Taking equation (23) into equation (17), one can get (24), as shown at the bottom of the this page.

Similarly, equation (24) is multiplied by $\left[\boldsymbol{J}_i^p\right]^H$ and $\left[\boldsymbol{J}_i^{S_1}\right]^H$, which results in (25), as shown at the bottom of the this page.

(3) The n_{th} total current $\boldsymbol{J}_i^{Tot(n)}$

Similar to the first order of SCBFs, the n_{th} order of SCBFs is defined as

$$\bar{\boldsymbol{Z}}_{ii}\boldsymbol{J}_i^{S^n} = -\sum_{i=1,j=1,i\neq j}^{M} \left|a_{(n-1)j}^{(n-1)}\right| \bar{\boldsymbol{Z}}_{ij}\boldsymbol{J}_j^{S^{n-1}} \tag{26}$$

where $\boldsymbol{J}_j^{S^{n-1}}$ is the $(n-1)_{th}$ order of SCBFs, and $a_{(n-1)j}^{(n-1)}$ is the coefficient of $\boldsymbol{J}_j^{S^{n-1}}$.

$$\begin{pmatrix} c_n^{L+2}+c_n^L & c_n^{L+3}+c_n^{L-1} & \cdots & c_n^{L+M+1}+c_n^{L-M+1} \\ c_n^{L+3}+c_n^{L+1} & c_n^{L+4}+c_n^L & \cdots & c_n^{L+M+2}+c_n^{L-M+2} \\ \vdots & \vdots & \vdots & \vdots \\ c_n^{L+M+1}+c_n^{L+M+1} & c_n^{L+M+2}+c_n^{L+M-2} & \cdots & c_n^{L+2M}+c_n^L \end{pmatrix} \begin{pmatrix} b_n^1 \\ b_n^2 \\ \vdots \\ b_n^M \end{pmatrix} = -2 \begin{pmatrix} c_n^{L+1} \\ c_n^{L+2} \\ \vdots \\ c_n^{L+M} \end{pmatrix} \tag{15}$$

$$\begin{bmatrix} \left[\boldsymbol{J}_1^p\right]^H \bar{\boldsymbol{Z}}_{11}\boldsymbol{J}_1^p & \left[\boldsymbol{J}_1^p\right]^H \bar{\boldsymbol{Z}}_{12}\boldsymbol{J}_2^p & \cdots & \left[\boldsymbol{J}_1^p\right]^H \bar{\boldsymbol{Z}}_{1M}\boldsymbol{J}_M^p \\ \left[\boldsymbol{J}_2^p\right]^H \bar{\boldsymbol{Z}}_{21}\boldsymbol{J}_1^p & \left[\boldsymbol{J}_2^p\right]^H \bar{\boldsymbol{Z}}_{22}\boldsymbol{J}_2^p & \cdots & \left[\boldsymbol{J}_2^p\right]^H \bar{\boldsymbol{Z}}_{2M}\boldsymbol{J}_M^p \\ \vdots & \vdots & \cdots & \vdots \\ \left[\boldsymbol{J}_M^p\right]^H \bar{\boldsymbol{Z}}_{M1}\boldsymbol{J}_1^p & \left[\boldsymbol{J}_M^p\right]^H \bar{\boldsymbol{Z}}_{M2}\boldsymbol{J}_2^p & \cdots & \left[\boldsymbol{J}_M^p\right]^H \bar{\boldsymbol{Z}}_{MM}\boldsymbol{J}_M^p \end{bmatrix} \begin{bmatrix} a_{p1}^{(p)} \\ a_{p2}^{(p)} \\ \vdots \\ a_{pM}^{(p)} \end{bmatrix} = \begin{bmatrix} \left[\boldsymbol{J}_1^p\right]^H \boldsymbol{V}_1 \\ \left[\boldsymbol{J}_2^p\right]^H \boldsymbol{V}_2 \\ \vdots \\ \left[\boldsymbol{J}_M^p\right]^H \boldsymbol{V}_M \end{bmatrix} \tag{21}$$

$$\begin{bmatrix} \bar{\boldsymbol{Z}}_{11}\boldsymbol{J}_1^p & \bar{\boldsymbol{Z}}_{12}\boldsymbol{J}_2^p & \cdots & \bar{\boldsymbol{Z}}_{1M}\boldsymbol{J}_M^p & \bar{\boldsymbol{Z}}_{11}\boldsymbol{J}_1^{S^1} & \bar{\boldsymbol{Z}}_{12}\boldsymbol{J}_2^{S^1} & \cdots & \bar{\boldsymbol{Z}}_{1M}\boldsymbol{J}_M^{S^1} \\ \bar{\boldsymbol{Z}}_{21}\boldsymbol{J}_1^p & \bar{\boldsymbol{Z}}_{22}\boldsymbol{J}_2^p & \cdots & \bar{\boldsymbol{Z}}_{2M}\boldsymbol{J}_M^p & \bar{\boldsymbol{Z}}_{21}\boldsymbol{J}_1^{S^1} & \bar{\boldsymbol{Z}}_{22}\boldsymbol{J}_2^{S^1} & \cdots & \bar{\boldsymbol{Z}}_{2M}\boldsymbol{J}_M^{S^1} \\ \vdots & \vdots & \vdots & \vdots & \vdots & \vdots & \vdots & \vdots \\ \bar{\boldsymbol{Z}}_{M1}\boldsymbol{J}_1^p & \bar{\boldsymbol{Z}}_{M2}\boldsymbol{J}_2^p & \cdots & \bar{\boldsymbol{Z}}_{MM}\boldsymbol{J}_M^p & \bar{\boldsymbol{Z}}_{M2}\boldsymbol{J}_1^{S^1} & \bar{\boldsymbol{Z}}_{M2}\boldsymbol{J}_2^{S^1} & \cdots & \bar{\boldsymbol{Z}}_{MM}\boldsymbol{J}_M^{S^1} \end{bmatrix} \begin{bmatrix} a_{p1}^{(1)} \\ a_{p2}^{(1)} \\ \vdots \\ a_{pM}^{(1)} \\ a_{11}^{(1)} \\ a_{12}^{(1)} \\ \vdots \\ a_{1M}^{(1)} \end{bmatrix} = \begin{bmatrix} \boldsymbol{V}_1 \\ \boldsymbol{V}_2 \\ \vdots \\ \boldsymbol{V}_M \end{bmatrix} \tag{24}$$

$$\begin{bmatrix} \left[\boldsymbol{J}_1^p\right]^H \bar{\boldsymbol{Z}}_{11}\boldsymbol{J}_1^p & \cdots & \left[\boldsymbol{J}_1^p\right]^H \bar{\boldsymbol{Z}}_{1M}\boldsymbol{J}_M^p & \left[\boldsymbol{J}_1^p\right]^H \bar{\boldsymbol{Z}}_{11}\boldsymbol{J}_1^{S^1} & \cdots & \left[\boldsymbol{J}_1^p\right]^H \bar{\boldsymbol{Z}}_{1M}\boldsymbol{J}_M^{S^1} \\ \vdots & \vdots & \vdots & \vdots & \vdots & \vdots \\ \left[\boldsymbol{J}_M^p\right]^H \bar{\boldsymbol{Z}}_{M1}\boldsymbol{J}_1^p & \cdots & \left[\boldsymbol{J}_M^p\right]^H \bar{\boldsymbol{Z}}_{MM}\boldsymbol{J}_M^p & \left[\boldsymbol{J}_M^p\right]^H \bar{\boldsymbol{Z}}_{M1}\boldsymbol{J}_1^{S^1} & \cdots & \left[\boldsymbol{J}_M^p\right]^H \bar{\boldsymbol{Z}}_{MM}\boldsymbol{J}_M^{S^1} \\ \left[\boldsymbol{J}_1^{S^1}\right]^H \bar{\boldsymbol{Z}}_{11}\boldsymbol{J}_1^p & \cdots & \left[\boldsymbol{J}_1^{S^1}\right]^H \bar{\boldsymbol{Z}}_{1M}\boldsymbol{J}_M^p & \left[\boldsymbol{J}_1^{S^1}\right]^H \bar{\boldsymbol{Z}}_{11}\boldsymbol{J}_1^{S^1} & \cdots & \left[\boldsymbol{J}_1^{S^1}\right]^H \bar{\boldsymbol{Z}}_{1M}\boldsymbol{J}_M^{S^1} \\ \vdots & \vdots & \vdots & \vdots & \vdots & \vdots \\ \left[\boldsymbol{J}_M^{S^1}\right]^H \bar{\boldsymbol{Z}}_{M1}\boldsymbol{J}_1^p & \cdots & \left[\boldsymbol{J}_M^{S^1}\right]^H \bar{\boldsymbol{Z}}_{MM}\boldsymbol{J}_M^p & \left[\boldsymbol{J}_M^{S^1}\right]^H \bar{\boldsymbol{Z}}_{M1}\boldsymbol{J}_1^{S^1} & \cdots & \left[\boldsymbol{J}_M^{S^1}\right]^H \bar{\boldsymbol{Z}}_{MM}\boldsymbol{J}_M^{S^1} \end{bmatrix} \begin{bmatrix} a_{p1}^{(1)} \\ \vdots \\ a_{pM}^{(1)} \\ a_{11}^{(1)} \\ \vdots \\ a_{1M}^{(1)} \end{bmatrix} = \begin{bmatrix} \left[\boldsymbol{J}_1^p\right]^H \boldsymbol{V} & \cdots & \left[\boldsymbol{J}_M^{S^1}\right]^H \boldsymbol{V}_M & \left[\boldsymbol{J}_1^{S^1}\right]^H \boldsymbol{V} & \cdots & \left[\boldsymbol{J}_M^{S^1}\right]^H \boldsymbol{V}_M \end{bmatrix}^T \tag{25}$$

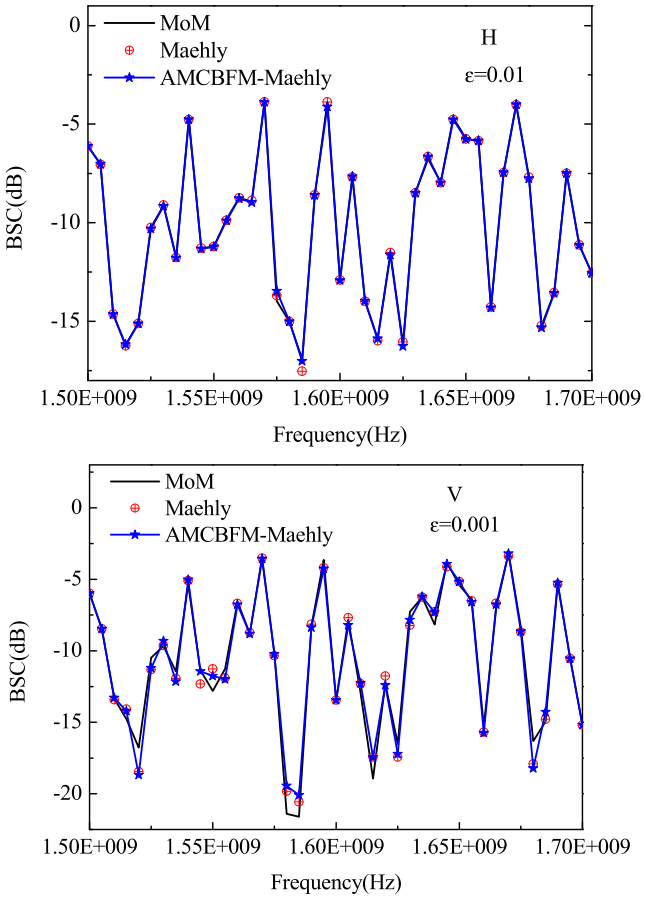

FIGURE 2. The BSC from rough surface obtained by the three different methods.

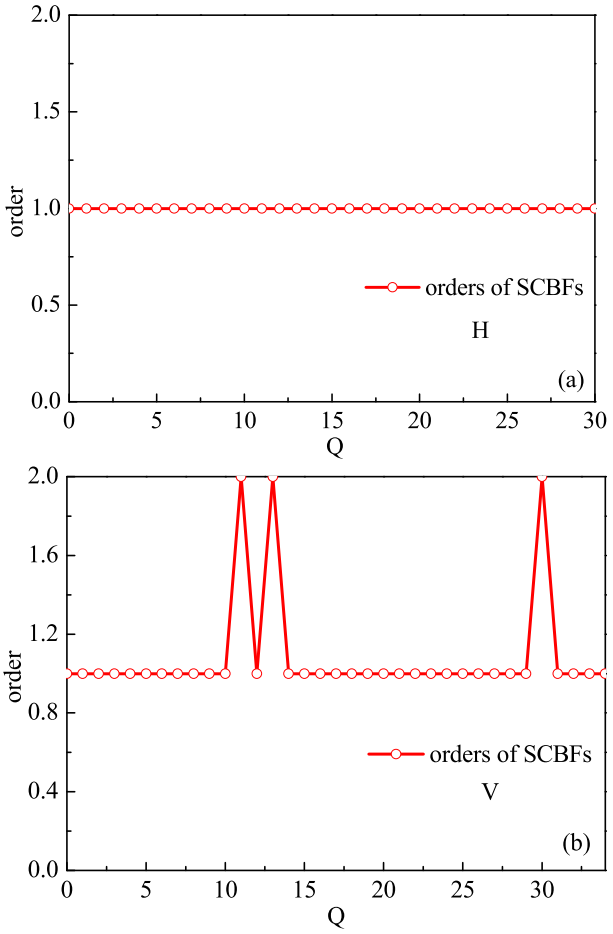

FIGURE 3. The order of the SCBFs of the hybrid AMCBFM-Maehly method at every Chebyshev node.

The n_{th} total current $\boldsymbol{J}_i^{Tot(n)}$ is defined as

$$\boldsymbol{J}_i^{Tot(n)} = a_{pi}^{(n)}\boldsymbol{J}_i^{p} + a_{1i}^{(n)}\boldsymbol{J}_i^{S^1} + \cdots + a_{ni}^{(n)}\boldsymbol{J}_i^{S^n} \tag{27}$$

(4) The current criterion

The current criterion that determines whether the higher-order of SCBFs are needed is defined as [17]

$$\varepsilon = \left| \frac{\left\|\boldsymbol{J}^{Tot(n+1)}\right\|_2 - \left\|\boldsymbol{J}^{Tot(n)}\right\|_2}{\left\|\boldsymbol{J}^{Tot(n+1)}\right\|_2} \right| \times 100\% \tag{28}$$

It is readily seen that the order of the SCBFs can be adaptively halted.

(5) The hybrid AMCBFM-Maehly method

After obtaining the induced electric current $J_n(k_i)$ along the rough surface at the Chebyshev nodes by the AMCBFM, the traditional Maehly technique is applied to get the rational function of the induced electric current along the rough surface over a frequency band.

III. NUMERICAL SIMULATIONS AND DISCUSSIONS

The validity and efficiency of the hybrid AMCBFM-Maehly method are firstly assessed by comparing its results with the results that were obtained by the MoM and the traditional Maehly technique. The BSC from a PEC Gaussian rough surface, as shown in Fig. 1, is calculated by these three methods. The incident angle is $\theta_i = 30°$, and the frequency responses with 0.005GHz increments over [1.5GHz, 1.7GHz] are simulated, i.e., $N_f = 41$. The root mean square height and the correlation length of the simulated Gaussian rough surface are $\delta = 0.04$m and $l = 0.2$m, respectively. The length of the simulated Gaussian rough surface is $L_s = 81.92$m with a discrete interval of $\Delta x = 0.02$m. In other words, there are $N = 4096$ segments along the rough surface. Thus, the dimensions of the MoM matrix and the traditional Maehly technique are 4096×4096. Here, the rough surface is equally divided into 4 cells, i.e. $N_i = 1024$ segments in every subcell. Therefore, the dimensions of the self-impedance matrix of the hybrid AMCBFM-Maehly method are only 1024×1024.

In Fig. 2, the current criteria of the AMCBFM-Maehly are set as $\varepsilon = 1\times10^{-2}$(H) and $\varepsilon = 1\times10^{-3}$(V), respectively. The BSC that are obtained through these three methods are shown. For the H polarization and the V polarized case, the orders of the rational function $L = M = 15$ and $L = M = 17$ are chosen, respectively. From Fig. 2, it is readily seen that the hybrid AMCBFM-Maehly method and the traditional Maehly technique agree well with the MoM in both H and V polarizations. Moreover, in Table 1, the CPU time of the hybrid AMCBFM-Maehly method, the traditional Maehly

TABLE 1. The CPU time of the hybrid AMCBFM-Maehly method, the traditional Maehly technique and the MoM.

Polarization	Method	CPU Time (seconds)	RMSE
H	MoM	502.054	---
	Maehly	348.187	1.0×10^{-2}
	AMCBFM-Maehly	290.625	8.938×10^{-3}
V	MoM	507.550	---
	Maehly	403.016	6.145×10^{-2}
	AMCBFM-Maehly	348.609	6.387×10^{-2}

technique, and the MoM are shown. It is obviously found that the hybrid AMCBFM-Maehly method costs less than half the CPU time of the MoM, and less than the Maehly technique.

Moreover, in Fig. 3, the orders of the SCBFs of the hybrid AMCBFM-Maehly method at every Chebyshev node are shown. For H polarization, the orders $L = M = 15$ are chosen, i.e. $Q \in [0, 30]$. For V polarization, the orders $L = M = 17$ are chosen, i.e. $Q \in [0, 34]$.

IV. CONCLUSION

In this paper, the hybrid AMCBFM-Maehly method was used to fast simulate the EM scattering from a one-dimensional PEC rough surface over a frequency band. Good agreement between the hybrid AMCBFM-Maehly method and the MoM was found. In addition, the AMCBFM-Maehly costs less than half the CPU time of the MoM. Furthermore, comparing with the traditional Maehly technique, the hybrid AMCBFM-Maehly approximation costs less time too.

In the future, this method will be expanded to solve the more realistic three-dimensional scattering problem. In addition, this method can also be applied to calculate the dielectric rough surface with a target located above it.

ACKNOWLEDGMENT

The authors would like to thank the reviewers for their constructive suggestions.

REFERENCES

[1] S. R. Chai and L. X. Guo, "A new fast algorithm based on compressive sensing for composite electromagnetic back scattering from a 2D ship located on a 1D rough sea surface," *Acta Phys. Sinica*, vol. 64, no. 6, 2015, Art. no. 060301.

[2] Y. Chen, D. Li, J. Hu, and J.-F. Lee, "A nonconformal surface integral equation for electromagnetic scattering by multiscale conducting objects," *IEEE J. Multiscale Multiphys. Comput. Techn.*, vol. 3, pp. 225–234, 2018.

[3] R. F. Harrington, *Field Computation by Moment Methods*. New York, NY, USA: IEEE Press, 1993, doi: 10.1109/9780470544631.ch3.

[4] Y.-W. Wei, L.-X. Guo, A.-Q. Wang, and Z.-S. Wu, "Application of multiregion model to EM scattering from a dielectric rough surface with or without a target above it," *IEEE Trans. Antennas Propag.*, vol. 61, no. 11, pp. 5607–5620, Nov. 2013.

[5] M. A. Moharram and A. A. Kishk, "Wideband electromagnetic scattering computations for smooth conducting 2D cylinders using the RAS-AWE method," in *Proc. 32nd Gen. Assem. Sci. Symp. Int. Union Radio Sci. (URSI GASS)*, 2017, pp. 1–4.

[6] M. A. M. Hassan and A. A. Kishk, "A combined asymptotic waveform evaluation and random auxiliary sources method for wideband solutions of general-purpose EM problems," *IEEE Trans. Antennas Propag.*, vol. 67, no. 6, pp. 4010–4021, Jun. 2019.

[7] R. Bao, A. Q. Wang, and Z. X. Huang, "Fast numerical simulations of electromagnetic scattering from one-dimensional rough surface over a frequency band," in *Proc. Progr. Electromagn. Res. Symp. (PIERS)*, Aug. 2016, pp. 4031–4035.

[8] R. Bao, A. Q. Wang, and Z. X. Huang, "Fast simulations of electromagnetic scattering from rough surface over a frequency band using asymptotic waveform evaluation technique: Horizontal polarization," *J. Electromagn. Waves Appl.*, vol. 32, no. 11, pp. 1379–1388, 2018.

[9] F. Kaburcuk and M. O. Kok, "Fast wideband solution using MBPE with MOM," in *Proc. Int. Appl. Comput. Electromagn. Soc. Symp. (ACES)*, Mar. 2017, pp. 1–2.

[10] W. Nie and Z. Wang, "Fast solutions of wide-band RCS of objects using general characteristic basis function method with the model based parameter estimation," in *Proc. Prog. Electromagn. Res. Symp. (PIERS)*, Aug. 2016, pp. 1160–1163.

[11] X. Wang, D. H. Werner, and J. P. Turpin, "Application of AIM and MBPE techniques to accelerate modeling of 3-D doubly periodic structures with nonorthogonal lattices composed of bianisotropic media," *IEEE Trans. Antennas Propag.*, vol. 62, no. 8, pp. 4067–4080, Aug. 2014.

[12] M. S. Chen, X. L. Wu, W. Sha, and Z. X. Huang, "Fast and accurate radar cross-section computation over a broad frequency band using the best uniform rational approximation," *IET Microw., Antennas Propag.*, vol. 2, no. 2, pp. 200–204, 2008.

[13] T. Song, L. Kuang, and Q. Liu, "Maehly approximation and phase extraction hybrid method for fast analysis of wideband electromagnetic scattering from a rough surface," in *Proc. Prog. Electromagn. Res. Symp. (PIERS)*, May 2017, pp. 2904–2907.

[14] R. Bao, A. Wang, and Z. Huang, "Fast frequency sweep analysis of a dielectric rough surface by Maehly approximation," *IEEE J. Multiscale Multiphysics Comput. Techn.*, vol. 2, pp. 224–227, 2017. [Online]. Available: https://ieeexplore.ieee.org/stamp/stamp.jsp?tp=&arnumber=8240582

[15] R. Bao, A. Q. Wang, and Z. X. Huang, "Wide-band EM scattering from multiple dielectric targets above a dielectric rough sea surface based on Maehly approximation," in *Proc. 7th IEEE Int. Symp. Microw., Antenna, Propag. EMC Technol. (MAPE)*, Oct. 2018, pp. 103–105.

[16] A. Q. Wang, R. Bao, and Z. X. Huang, "Application of Maehly approximation to EM scattering from a dielectric rough surface and a dielectric object over a frequency band," in *Proc. Int. Appl. Comput. Electromagn. Soc. Symp. China (ACES)*, Jul./Aug. 2018, pp. 1–2.

[17] G. D. Han and C. Q. Gu, "Adaptively modified characteristic basis function method for electromagnetic scattering study," *J. Electron. Inf. Technol.*, vol. 30, no. 10, pp. 2364–2368, 2008.

[18] J. J. Wang, A. Q. Wang, Z. X. Huang, and T. Z. Jiang, "A fast algorithm for electromagnetic scattering from one-dimensional rough surface," *Int. J. Antennas Propag.*, vol. 2019, Apr. 2019, Art. no. 7985421.

[19] L. Tsang and J. A. Kong, *Scattering of Electromagnetic Waves: Numerical Simulations*. New York, NY, USA: Wiley, 2001, pp. 111–176.

[20] G. Han and C. Gu, "A hybrid QR factorization with dual-MGS and adaptively modified characteristic basis function method for electromagnetic scattering analysis," *Microw. Opt. Technol. Lett.*, vol. 49, no. 11, pp. 2879–2883, 2007.

ANQI WANG was born in Anhui, China, in 1986. She received the B.S. and Ph.D. degrees from Xidian University, Xi'an, China, in 2007 and 2013, respectively. Her current research interests include computational electromagnetics, and the electromagnetic wave scattering characteristics of rough surface and targets.

JINGJING WANG was born in Anhui, China, in 1993. She received the M.S. degree from the School of Electronics and Information Engineering, Anhui University, China, in 2019. She is currently pursuing the Ph.D. degree in radio science with the School of Physics and Optoelectronic Engineering, Institute of Radio Propagation, Xidian University, China. Her research interests include applied and computational electromagnetics for remote sensing from target above or below random rough surfaces.

ZHIXIANG HUANG was born in Anhui, China, in 1979. He received the B.S. and Ph.D. degrees from Anhui University, Hefei, China, in 2002 and 2007, respectively. He was a Visiting Scholar with Iowa State University, USA, from September 2010 to September 2011. From August 2013 to October 2013, he was a Visiting Professor with The University of Hong Kong. From February 2014 to February 2015, he was a Visiting Professor with the Beijing National Laboratory for Condensed Matter Physics, Institute of Physics, Chinese Academy of Sciences. He has published one monograph on the symplectic finite-difference time-domain method and two book chapters at CRC Press and In Tech Publishers. He has published 60 peer-reviewed journal articles included in the Web of Science Core Collection. His current research interests include time-domain numerical methods, metamaterials, and active metamaterials. He is a member of the OSA. In 2015, he was awarded the Second Prize of Science and Technology from the Anhui Province Government, China, and the National Science Foundation for Outstanding Young Scholar of China, in 2017.

LIXIN GUO (S'95–M'03–SM'16) received the M.S. degree in radio science from Xidian University, Xi' an, China, in 1993, and the Ph.D. degree in astrometry and celestial mechanics from the Chinese Academy of Sciences, China, in 1999. From 2001 to 2002, he was a Visiting Scholar with the School of Electrical Engineering and Computer Science, Kyungpook National University, Daegu, South Korea. He has also been a Visiting Professor with the d'Energetique des Systemes et Precedes, University of Rouen, Mont-Saint-Aignan, France, and a Faculty Member of engineering and physical sciences with The University of Manchester, Manchester, U.K. He is currently a Professor and the Head of the School of Physics and Optoelectronic Engineering, Xidian University. He was a Distinguished Professor of the Changjiang Scholars Program, in 2014. He has been the Chief Professor of the Innovative Research Team, Shaanxi, China, since 2014. He has authored or coauthored four books and over 300 journal articles. He has been the in charge of and undertaken more than 30 projects. His research interests include electromagnetic wave propagation and scattering in complex and random media, computational electromagnetics, inverse scattering, antenna analysis, and design. He was a recipient of the National Science Fund for Distinguished Young Scholars, in 2012.

TIEZHEN JIANG, photograph and biography not available at the time of publication.